Structures and Cytotoxic Properties of Trichoverroids and Their Macrolide Analogues Produced by Saltwater Culture of *Myrothecium verrucaria*

Taro Amagata,[†] Christopher Rath,[†] Jérôme F. Rigot,[†] Nick Tarlov,[†] Karen Tenney,[†] Frederick A. Valeriote,[‡] and Phillip Crews*[,†]

Department of Chemistry and Biochemistry and Institute for Marine Sciences, University of California−Santa Cruz, Santa Cruz, California 95064, and Josephine Ford Cancer Center, Detroit, Michigan 48202

Received February 21, 2003

Saltwater culture of *Myrothecium verrucaria*, separated from a *Spongia sp*. collected in Hawaii, was a source of three new trichothecenes, 3-hydroxyroridin E (**1a**), 13′-acetyltrichoverrin B (**2**), and miophytocen C (**3**) and nine known related compounds (**1b**, **4**, **5**, **6**, **7a**, **7b**, **8**, **9a**, and **9b**). The stereostructures of the new compounds were established on the basis of 1D and 2D NMR spectral analyses and a chemical transformation. At the same time, the stereostructures of known compounds, **1b**, **4**, and **5** reported previously were also elucidated. All the compounds except **3** showed significant cytotoxicity against murine and human tumor cell lines. Moreover, the structure−activity relationships (SARs) were established from the results of the bioassay data.

Introduction

In the early 1990s we hypothesized that chemically prolific sponges could provide filamentous fungi whose saltwater culture would produce diverse secondary metabolites. Two early findings key to validating this idea included Kitagawa's isolation of trichoharzin[1] from culture of a *Mycale* sponge-derived salt obligate strain *Trichoderma harzianum*, and our report of the chloriolins A−C[2] produced during the saltwater culture of an unidentified fungus from *Jaspis splendens*. Further research along these lines was begun in many laboratories and has resulted in a host of significant additional discoveries. For example, we subsequently described unique structures of sponge-derived fungal metabolites such as the chlorocarolides A and B,[3] obtained from saltwater cultures of *Aspergillus*, asperazine[4] isolated from another *Aspergillus* strain, and epoxysorbicillinol[5] derived from *Trichoderma longibrachiatum*. The ensuing parallel discoveries by others included the gymnastatins from *Gymnasella dankaliensis* reported by Amagata and Numata,[6] the petrosifungins from a *Penicillium*[7] described by Bringmann, the aspergillones from *Aspergillus* disclosed by Ebel and Proksch,[8] and the pandangolides outlined by Bernan and Ireland.[9]

Many marine-derived fungi seem to produce analogues of those previously discovered from terrestrial fungi.[10] However, the recent literature shows promise for new opportunities such as obtaining and culturing sponge-derived biota not previously described,[11] or gaining access to strains capable of producing compound classes identical to those isolated from the sponge itself.[12]

In recent years we have turned our attention to mining our library of sponge-derived fungi for new cytotoxic compounds possessing selectivity to solid tumor cell lines. The library is now greater than 1000 strains and provided the platform for the research reported below. We began with the straightforward precept that certain of these strains would produce, under saltwater culture condition, active extracts, and this could be followed up with the bioassay-guided isolation to yield significant compounds. Thus, an extensive effort was begun to validate our ideas and obtain chemotypes that would be candidates for further pharmacological follow up. To achieve this end we have evaluated 1670 extracts from 817 fungi to probe for their in vitro selectivity, potency, or both in a screen consisting of a disk diffusion soft agar assay using a panel of five cancer cell lines (solid tumors and leukemias) and two normal cells.[13] A high priority was given to the potent extracts (1%) and to the solid tumor selective extracts (1.9%). Also, extracts containing complex compounds were emphasized, and the final step involved both molecular-based and traditional approaches to taxonomy to foreshadow the type of metabolites expected during the bioassay-guided isolations. A combination of these approaches focused our attention on a fungus obtained from *Spongia* sp. collected in Hawaii. This fungal isolate was robust in its growth during saltwater culture, and it provided crude extracts that were among the most potent of any in our library in the disk diffusion soft agar cytotoxicity assay. Preliminary analysis by mass spectrometry indicated the presence of complex mixtures of compounds with MW's > 500 amu. The producing organism was identified as *Myrothecium verrucaria*, and eventually we isolated and characterized 12 trichoverroids or their macrolide analogues from the culture samples.

Strains of *Myrothecium verrucaria* and its related taxa, *Myrothecium roridum*, have been intensely studied by Jarvis and others for their content of the trichothecene class of sesquiterpenes and their macrocyclic analogues.[14] Trichothecenes are highly functionalized sesquiterpenes based on the tetracyclic core shown in Chart 1 and can be further categorized, by expanding

* To whom correspondence should be addressed. Tel.: (831) 459-2603. Fax: (831) 459-2935. E-mail: phil@chemistry.ucsc.edu.
[†] University of California−Santa Cruz.
[‡] Josephine Ford Cancer Center.

10.1021/jm030090t CCC: $25.00
Published on Web 08/23/2003

Chart 1. Structual Family of Trichothecenes

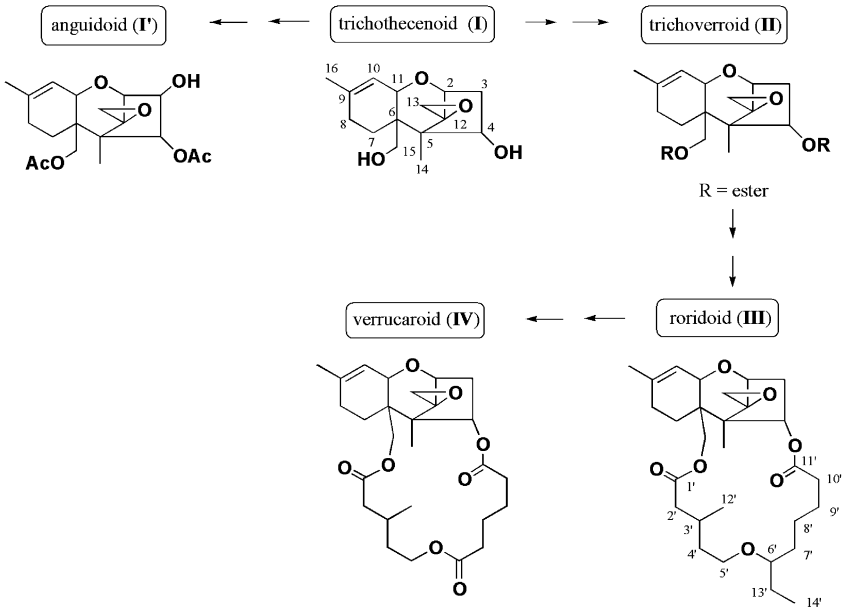

on Jarvis's nomenclature,[15] as a trichothecenoid (**I**) or anguinoid (**I′**), a trichoverroid (**II**), a roridoid (**III**), and a verrucaroid (**IV**). Most trichothecenes possess an epoxide ring at C12−13, which appears to be critical for bioactivity, including antiproliferating action,[16] ability to induce apoptosis,[17] antimalarial activity,[18] and antiviral effects.[19] Alternatively, there are few examples of 12,13-deoxytrichothecenes.[20] Interest in the trichothecenes continues because of their biological activity,[21] the challenge associated with their total synthesis,[22] curiosity about their biosynthesis,[23] and the possibility for the re-engineering of their biosynthetic pathways.[24]

Myrothecium verrucaria cultured in this study was a source of three new trichothecenes (**1a**, **2**, and **3**), together with nine related known compounds—roridin L (**1b**),[25] roridin M (**4**),[25] verrucarin M (**5**),[25] verrucarin A (**6**),[26] roridin A (**7a**),[26] isororidin A (**7b**),[27] epiroridin E (**8**),[15a] trichoverrin A (**9a**),[28] and trichoverrin B (**9b**).[28] We describe herein the structure elucidation of three new compounds (**1a**, **2**, and **3**) and the unreported stereochemistry of three previously published compounds (**1b**, **4**, and **5**). The cytotoxicity properties of these and other analogues are evaluated and discussed, and we consider the possibility for further development of these compounds as therapeutic leads.

Results and Discussion

When this project was initiated, there were not any known reports of marine-derived *Myrothecium*. However, during the course of our work, a paper appeared describing two type **III** and two type **IV** analogues from *M. roridum* obtained from submerged wood obtained in Palau[20e,29] (see the summary of Table S1). The culture broth extracts of the fungus, *M. verrucaria* (strain no. 973023) separated from *Spongia* sp. (coll. no. 97103), collected off the coast of Maui, showed potent activity against murine lymphocytic leukemia L1210 and human colon tumor H116 cell lines in the soft agar-based bioassay system. The ^{1}H NMR spectrum of the extract used for the screening contained characteristic signals of type **II**−**IV** trichothecenes including two singlet methyls (δ_H 0.8, 1.8), an epoxide (δ_H 2.2, 2.8), ester groups (δ_H 3.2), and a double bond (δ_H 5.6−8.0). Furthermore, the ESI-TOFMS showed many peaks around *m/z* 500−600, consistent with the molecular weight range of such compounds. To perform comprehensive investigation of the structures and bioactivities of the fermentation products, this strain was recultured (12 L, 28 °C) at 150 rpm for 21 days in a medium containing 1.5% malt extract broth in filtered Monterey Bay seawater adjusted to pH 7.3. The CH_2Cl_2 solubles obtained from the EtOAc extract of the culture filtrate was purified by bioassay-guided fractionation employing silica gel flash column chromatography. Final isolation of the active components was performed by reversed-phase HPLC to yield three new compounds, 3-hydroxyroridin E (**1a**), 13′-acetyltrichoverrin B (**2**), and miophytocen C (**3**), and nine related known compounds (as outlined in Chart S1).

The molecular formula of 3-hydroxyroridin E (**1a**) and an accompanying metabolite roridin L (**1b**) eventually assigned as the 6′-epimer of **1a** were both determined to have the formula $C_{29}H_{38}O_9$ from HRESI-TOFMS data. The structure elucidation of this pair was begun by dereplication using the molecular formula and the features of the trichothecene **I** core skeleton as database search seeds.[30] On the basis of comparison to literature spectral data,[25] **1b** was shown to be identical to roridin L, whose stereochemistry had not yet been described. Alternatively the properties of **1a** did not correspond to those of any known trichothecene. However, the NMR data of **1a** closely matched that of **1b** (Table S5), enabling the characterization of the 2D structure to proceed in a straightforward manner. The analyses of ^{1}H−^{1}H gCOSY and gHMBC for **1a** gave three substructures as shown in Figure 1. Substructure **A** based on the sesquiterpene core of **I** was recognized from ^{1}H−^{1}H NMR COSY correlations (C2−C4, C7−C8, and C10−C11) and the gHMBC correlations (H2/C11, 12, and 13, H4/C6 and C12, H7/C6, 9, and 11, H8/C6, 9, and 10, H10/C6, 8, and 16, H13a and H13b/C12, H14/C4, 5, 6, and 12, H15/C5, 6, 7, and 11, and H16/C8, 9 and 10).

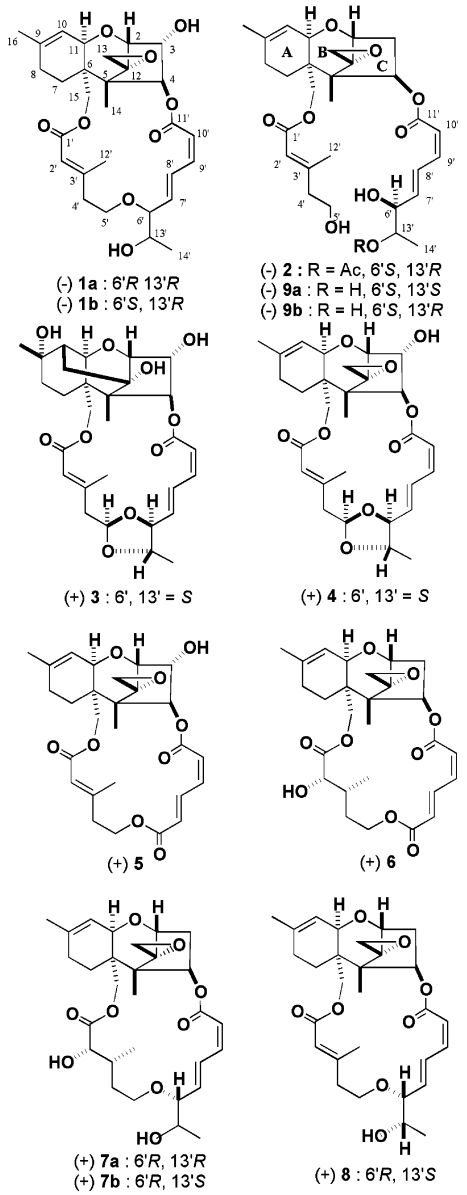

Substructure **B** was assembled from ^{1}H−^{1}H gCOSY correlations (C4′−C5′) and gHMBC correlations (H2′/C1′, 4′ and 12′, H4′/C2′, 3′ and 12′ and H12′/C2′, 3′ and 4′). The last substructure **C** was also justified from the ^{1}H−^{1}H gCOSY correlations (C14′-C13′-C6′-C10′) and an HMBC correlation (H9′/C11′). Last, these substructures were connected together using additional gHMBC correlations (H4/C11′, H15/C1′, and H5′/C6′) also shown in Figure 1. Thus, the structure proposed had to be a diastereomer of **1b**.

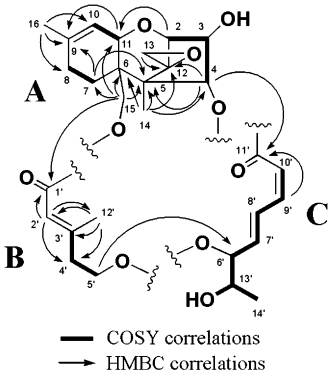

Figure 1. ^{1}H−^{1}H gCOSY and gHMBC NMR selected correlations for **1a**.

Table 1. Diagnostic ^{1}H NMR Parameters That Define the Macrocyclic C6′ and Side Chain Absolute Configuration

compd	H13′ multiplicity	$^3J_{6',7'}$ (in Hz)	^{13}C $\Delta\delta_{7,8}$	configuration
1a	quintet	3.0	11.7	6′*R*, 13′*R*
1b	dq	7.8	2.9	6′*S*, 13′*R*
8	qd	3.2	10.9	6′*R*, 13′*S*
13[a]	five-line multiplet	3	11.5	6′*R*, 13′*R*
14[a]	five-line multiplet	6	4.2	6′*S*, 13′*S*
15[a]	eight-line multiplet	6	3.7	6′*S*, 13′*R*

[a] Data from the litrature.[15a]

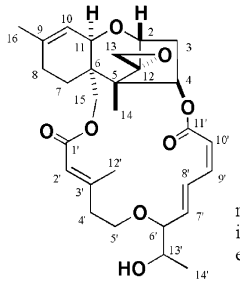

roridin E (**13**); 6′*R* 13′*R*
isororidin E (**14**); 6′*S*, 13′*S*
epiisororidin E (**15**); 6′*S*, 13′*R*

The relative chemistry of the trichothecene ring substituents in both **1a** and **1b,** excepting that at C3, was assigned on the basis of NOESY correlations (H2/H13b, H4/H11 and 15b, H11/H15a, and H13a/H14). The geometries of the two disubstituted double bonds in the macrocyclic ring were deduced from coupling constants ($^3J_{7',8'}$ ∼15 Hz, and $^3J_{9',10'}$ ∼11 Hz) of olefinic protons and the carbon chemical shift (δ ∼19.5) of the allylic methyl (C12′), as supported by NOESY, was used to assign the *E*-arrangment of the trisubstituted double bond. Next, the orientation of the hydroxyl group at C3 on **1a** and **1b** was considered. The coupling constants to H3 on **1a** and **1b** were identical as $^3J_{2,3}$ 4.9 Hz and $^3J_{3,4}$ 3.4 Hz, indicating an identical OH group stereochemistry for both compounds. Final assessment of this stereochemistry was made by reference to coupling constant data of trichothecinols A−C (**10**−**12**)[31] (see Table S6). Namely, the coupling constants to H3β and H3α show a diagnostic pattern (H3β: $^3J_{2,3\beta}$ ∼ 5.0 Hz, $^3J_{3\beta,4}$ ∼ 3.5 Hz; H3α: $^3J_{2,3\alpha}$ 0 Hz, $^3J_{3\alpha,4}$ 7.8 Hz). Therefore, applying this trend to the data of **1a** and **1b** further confirms that the hydroxyl groups in each are in an α orientation. Since the absolute stereochemistry of **10**−**12** has also been reported,[31] by analogy to their common biosynthetic origin, the seven chiral centers on the trichothecene ring of **1a** and **1b** can be assigned as 2*R*, 3*S*, 4*S*, 5*S*, 6*R*, 11*R*, 12*S*.

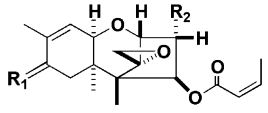

10: R_1 = O, R_2 = OH
11: R_1 = α-OH, β = H, R_2 = H
12: R_1 = α-OH, β = H, R_2 = OH

The remaining stereochemistry at C6′ and C13′ of **1a** and **1b** was determined by the employing diagnostic ^{1}H NMR parameters summarized in Table 1 for the H13′ multiplet, for the coupling constants to H6′ and for the ^{13}C chemical shifts at C7′ and C8′. Recently, Jarvis used

such considerations to assign the absolute stereochemistry at C6′ and C13′ in several roridin E diastereomers, **8**, **13**, **14**, and **15**),[15a] using the following patterns. First, a five-line multiplet was observed at H13′ for threo configuration (6′ and 13′ = *R*, *R* or *S*, *S*), versus an eight-line multiplet at H13′ for the erythro configuration (6′*R*, 13′*S* or 6′*S*, 13′*R*). Second, epimers having *R*-C6′ exhibit $^3J_{6',7'} \sim 3$ Hz and $\Delta\delta_C$ C7′−C8′ ∼ 12 ppm, versus epimers having *S*-C6′ (*S*) show $^3J_{6',7'} \sim 6$ Hz and $\Delta\delta_C$ C7′−C8′ ∼ 4 ppm. The properties for **1a** included an H13′ five-line multiplet, indicating C6′ and C13′ were threo (6′*R*, 13′*R* or 6′*S*, 13′*S*), along with $^3J_{6',7'}$ 3.0 Hz and $\Delta\delta_C$ C7′−C8′ 11.7 ppm, both indicating a 6′*R* configuration. Consequently, C6′ and C13′ were both assigned as *R*, completing the absolute structure of **1a**. Using this same approach to analyze **1b**, its stereochemistry was determined to be 6′*S* and 13′*R*. The complete stereochemistry of (−) roridin L (**1b**) has now been assigned as shown herein.

Attention shifted to the characterization of 13′-acetyltrichoverrin B (**2**). Its molecular formula was established as $C_{31}H_{42}O_{11}$ by HRESI-TOFMS. Database searches using this molecular formula plus the sesquiterpene core of **I** as search queries did not afford any hits. The next step was to repeat the searches with the OAc (δ_H 2.05, s, *A* = 3) group subtracted from the MF to provide a search formula of $C_{29}H_{40}O_9$. This yielded several hits including: roridin A (**6**), isororidin A (**9**), trichoverrins A (**9a**) and B (**9b**), and isotrichoverrins A and B (C9′-C10′ *E* isomer of **9a** and **9b**). Sifting through this list was accomplished by employing the entire set of ^{1}H and ^{13}C NMR data of **2** shown in Table S7 and revealed the similarity in the properties of **2** to **9a** and **9b**. Therefore, this new compound was deduced as being a monoacetate of **9a** or **9b** and was supported by the HMBC correlations, which allowed the acetyl group to be connected at C13′ (HMBC correlation from H13′ to *C*OCH$_3$). The stereochemistry in the sesquiterpene ring of **2** was assumed to be identical to that of **1a** due to their common biosynthetic origin. This assumption also supported the NOESY data (Table S7). The NMR data was then used in an analogous fashion as described above to set the geometry of the three double bonds in the two ester residues. Similarly, by analogy to the pattern observed by Jarvis in characterizing **9a** and **9b**,[15b] the diagnostic pattern of an eight-line multiplet at H13′ indicated erythro configuration (*S*, *R* or *R*, *S*) at C6′ and C13′ in **2**. To finalize this assignment, **2** was deacetylated under weakly basic conditions. The product displayed a five-line multiplet (quint) splitting pattern of H7′ which meant that the product had a threo configuration (C6′ = C13′ = *S* or *R*). Assuming that the reaction proceeded by inversion at C13′, accompanied by anchiomeric assistance from the OH at C6′, explained this result. Further inspection of the physical properties of the reaction product including ^{1}H and ^{13}C NMR spectra and optical rotation indicated it was identical to known **9a**. Working backward then allowed the stereochemistry in **2** to be assigned as *S* at C6′ and *R* at C13′, respectively. Therefore, the absolute structure of (−) **2** was determined as 2*R*, 3*S*, 4*S*, 5*S*, 6*R*, 11*R*, 12*S*, 6′*S*, and 13′*R*.

The last structure to be characterized was miophytocen C (**3**) whose molecular formula, $C_{29}H_{38}O_{10}$, was

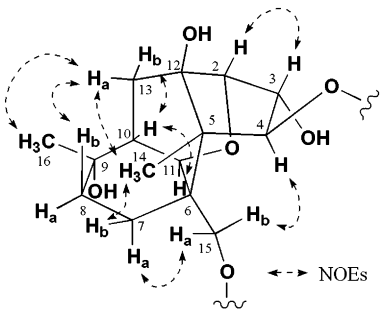

Figure 2. Selected NOESY correlations of trichothecene ring of **3**.

deduced from HRESI-TOFMS data. Early on it was recognized that **3** was missing the epoxide group normally observed in a trichothecene ring at C12′-C13′. In addition, the NMR data (Table S8), intimated that this compound also possessed a hemiacetal group (δ_H 5.67, δ_c 101.7). Comparing the NMR data of **3** to that of both **1a** and 8-acetoxyroridin H (**16**) facilitated completing its structure elucidation. First, it was evident from both ^{1}H and ^{13}C NMR data (*J*'s and δ's) that **3** and **1a** possessed B/C-rings identical in structure and stereochemistry. However, the A-rings were different, and as noted above the epoxide was missing. The major change in NMR data for the A-ring was that the signals for the double bond at C9−10 were missing and were replaced by a quaternary carbon (δ_C 73.5, s) having an attached oxygen. HMBC correlations revealed that this carbon was also adjacent to an sp^3 methine (δ_H 2.26, δ_C 43.8). One missing signal for the epoxide was replaced by a quaternary carbon (δ_C 78.1, s) bearing an attached oxygen. The second missing peak was identified from HMBC correlations as an adjacent sp^3 methylene (δ_C 29.4, t; δ_H 1.45, 1.88, ^2J = 13.7 Hz). Additional new HMBC correlations in **3** and not previously observed for **1a** consisted of those from H13a to C2, 5, 9, 10, and 12 and from H13b to C2, 9, 10, 11, and 12. These data supported the formation of a new carbocyclic ring via connection from C10−C13. This feature also explained the additional vicinal coupling observed between their respective protons. In addition, these data justified locating C10 adjacent to C9, the carbon with the attached tertiary oxygen. Last, hydroxyl groups were assigned at C9 and C12, and they were deduced to be both α supported by NOESY correlations (H13a/H14 and 16, H13b/H10). These correlations along with the additional data summarized in Figure 2 further justifies the stereochemistry assigned for the tetracyclic sesquiterpenoid portion of the structure. Comparing the remaining NMR data of **3** to that of 8-acetoxyroridin H (**16**)[32] whose structure is based on single-crystal X-ray

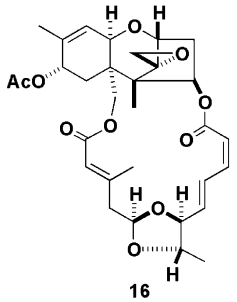

16

analysis revealed that their macrocylic rings and fea-

Table 2. Zone Unit Differentials in the Disk Diffusion Soft Agar Colony Formation Assay[a]

				murine tumor selectivity[d]			human tumor selectivity[d]	
compd	type	(μg/mL)[b]	relative activity[c]	Z_{C38}-Z_{L1210}	Z_{C38}-Z_{CFU-GM}	Z_{L1210}-Z_{CFU-GM}	Z_{H116}-Z_{CEM}	Z_{H125}-Z_{CEM}
1a	**III**	0.14	392	−300	−50	250	0	50
1b	**III**	1.3	632	−400	0	400	−100	−50
2	**II**	31	9	−400	−100	300	−150	400
3	**III**	550	1	−350	−50	300	−50	−50
4	**III**	41	14	0	100	100	−150	−100
5	**IV**	30	19	150	−50	−200	−50	−50
6	**IV**	0.78	692	−300	50	350	−200	−200
7a	**III**	0.78	703	−300	50	350	−100	−150
7b	**III**	0.90	1066	−500	−50	450	−150	−150
8	**III**	8.6	256	−550	0	550	>−150	>−50
9a	**II**	163	3	−500	−200	300	−50	−100
9b	**II**	175	6	−300	300	600	−150	−100
17	**I′**	0.24	423	−150	0	150	−100	0

[a] Measured in zone units.[13] Murine cell lines: L1210 (lymphocytic leukemia), C38 (colon adenocarcinoma), CFU-GM (normal bone marrow), Human cell lines: H116 (colon tumor), H125 (lung nonsmall cell carcinoma), CEM (lymphocytic leukemia) CFU-GM (normal bone marrow). [b] Concentration (15 μL applied to disk) to give 500 zone units against H116. [c] Relative activity against H116 is calculated by setting compound **3** as 1.0. The relative activity (RA) is calculated by the following formula; RA = dilution required for 500 zone units × 100/mg/mL. [d] Significant selectivity is defined by a difference of >250 zone units.

tures of stereochemistry were identical. Therefore, the absolute structure of **3** was deduced to be 2*R*, 3*S*, 4*S*, 5*S*, 6*R*, 9*S*, 10*S*, 11*R*, 12*R*, 6′*S*, and 13′*S*.

The eight additional compounds dealt with in this study were known, but two were published without comprehensive assignment of their stereochemical features. The latter group consists of **(+)** roridin M (**4**)[25] and (+) verrucarin M (**5**)[25] whose published properties did not include optical rotation data. These compounds were carefully analyzed on purification, and their NMR data are shown in Table S9. This information provided the justification for the absolute stereochemistry depicted here for **4** and **5**, and the logic employed to arrive at this assignment was analogous to that outlined above in the characterization of **1b**. For example, the trichothecene ring and geometry of the double bonds on **4** and **5** were determined to be the same as **1a** from the NOESY data (Table S9). The hydroxyl group at C3, for both **4** and **5**, was also determined as α-OH (Table S6). In summary, the absolute structures of **4** and **5** were determined as 2*R*, 3*S*, 4*S*, 5*S*, 6*R*, 5′*S*, 6′*S*, and 13′*R* and 2*R*, 3*S*, 4*S*, 5*S*, 6*R*, 11*R*, and 12*S*, respectively.

The cytotoxic properties of all the compounds obtained in this study were assessed against murine and human tumor cell lines using the disk diffusion soft agar colony formation assay.[13] To calibrate our findings, it is first necessary to briefly review literature data dealing with the cytotoxicity and antitumor and anticancer evaluation of trichothecenes. Highlights of this SAR appear in Chart S2 and reflect substantial in vivo data collected in the early 1980s from the P388 leukemia mouse model on 61 anguidoid (**I′**)[33] analogues and on 37 type **III** and **IV** macrocycles.[21] The positive in vivo activity in the mouse for anguidin (**17**)[34] prompted, in the late 1970s,

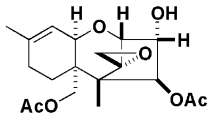

17

five distinct series of Phase II studies that involved a total of 484 patients.[35] Unfortunately each of the studies, where anguidin was used as a single agent, was discontinued because of varied toxicity effects and the lack of substantive antitumor activity. Very recently, between 2001 and 2002, four different research teams have reported on the in vitro cytotoxicity properties of type III and IV tricothecenes (Chart S1).[25,29a,33,36] However, missing from this list are in vitro cytotoxicity data for both type I and type II analogues. The most important universal SAR trends evident include: (a) the C12−C13 epoxide is required for vigorous activity (IC_{50} < 1 nM), (b) mixed effects are observed when a C9−C10 epoxide is introduced, (c) the incorporation of a 3-keto, or 8-keto, or a C16-hydroxide can enhance activity, and (d) trichoverroids (**II**) are minimally toxic to normal cells such as NIH3T3.[37]

All the compounds showed significant inhibition zones against all cell lines in our bioassay system.[13b] Many, in fact, demonstrated leukemia selectivity as shown in Table 2 by the large negative zone differentials between L1210 leukemia and both Colon38 and the positive zone differentials between Colon38 and CFU-GM. An estimate of the potency of each compound was also obtained and shown in Table 2 as relative activity. Consistent with the trends discussed above, miophytocene C (**3**) is the least potent compound because the critical C12−C13 epoxide residue is absent. Also, the three trichoverroids (type **II** compounds) were all weak in their relative activity and the same was true for the epoxide containing roridoid **4**, a roridoid possessing both the 12,13-epoxide and a 1,3-dioxalane ring embedded in the macrocycle. Although anguidine (**17**)[38] was intermediate in its relative activity, it was unselective against both murine and human tumors. Alternatively, compounds in the most active group [**7b** > **7a**, ≈ **6**, **1b** > **1a** > **8**] were all 12,13-epoxy containing macrocyclic trichothecenes as either roridiods (**III**) or verrucaroids (**IV**). In addition, the best murine tumor selectivity and relative activity is associated with the presence of a 2′-OH substituent on the macrocyclic ring of either a roridoid (**III**) or a verrucaroid (**IV**). Finally, the stereochemistry at C6′-C13′ also plays a role in affecting both selectivity and potency. The favored arrangement was 6′*R*, 13′*S* for the **7a****7b** pair and 6′*S*, 13′*R* for the **1a****1b** pair.

All the compounds except **8** were also evaluated in the NCI 60 cell line screen,[39] and the data obtained is shown in Table 3. As above, anguidine (**17**) was also

Table 3. Selected NCI-DTP[a] Antitumor Activity Results against in Vitro 60-Cell Lines Data (IC_{50}, μM[b])

tumor type	**1a** NSC 724381[d]	**1b** NSC 720909	**2** NSC 720697	**3** NSC 722594	**4** NSC 720694	**5** NSC 720693	**6** NSC 720162	**7a**[c] NSC 200737	**7b** NSC 720910	**9a** NSC 720696	**9b** NSC 720695	**17**[c] NSC 141537
leukemia												
CCRF−CEM	-[e]	-	-	-	-	-	-	-	-	-	-	<0.001
HL-60 (TB)	0.010	-	-	-	-	-	-	-	-	-	-	<0.001
MOLT-4	-	-	-	-	-	-	-	-	-	-	-	<0.001
NSCL												
A549/ATCC	nd	-	9.77	-	-	nd	-	-	-	5.44	6.21	<0.001
NCI−H226	0.007	0.091	4.87	-	0.157	0.033	0.004	0.003	nd	8.41	6.93	<0.001
NCI−H522	-	0.021	1.21	-	0.026	<0.001	<0.001	<0.001	0.095	0.936	0.904	<0.001
colon												
COLO205	-	0.013	0.612	-	nd	0.007	<0.001	0.003	0.008	1.31	4.02	<0.001
HCT-116	<0.001	-	-	-	0.075	nd	-	-	-	-	-	<0.001
HCT-15	-	-	-	-	0.483	0.073	8.10	-	-	-	-	<0.001
melanoma												
M14	<0.001	0.024	9.0	-	0.075	0.008	<0.001	<0.001	0.010	7.87	7.10	<0.001
SK-MEL-2	-	0.024	-	-	0.260	0.037	0.008	0.003	-	7.54	8.91	<0.001
UACC-62	0.009	0.018	9.56	-	0.409	0.057	0.005	0.005	0.002	-	-	<0.001
renal												
786-0	0.059		-	-	-	-	nd	0.040	-	-	-	<0.001
A498	0.009	0.019	2.38	-	0.583	0.053	0.003	0.316	0.006	6.96	8.16	<0.001
RXF 393	0.057	-	-	-	2.18	0.084	-	0.002	0.010	-	-	<0.001
breast												
MCF7	-	-	-	-	-	-	1.20	-	-	-	-	<0.001
MDA-MB-435	0.004	0.020	2.26	-	0.137	0.014	0.004	0.006	0.031	2.70	5.49	<0.001
MDA-N	nd	0.021	5.08	-	0.083	0.014	0.082	0.003	0.008	7.78	-	<0.001

[a] Data provided by the National Cancer Institute-Development Therapeutics program (NCI-DTP). [b] $IC_{50} = LC_{50}$ single point data reported on the website given above. [c] These data were quoted from NCI's online data. [d] For the comprehensive data set against 60 cell lines use the NSCs above at http://dtp.nci.nih.gov/. [e] −: inactive ($IC_{50} > 10$ μM). nd: no data.

used as an important standard, and in contrast to the data of Table 2 it was observed to be the most potent. As expected, miophytocen C (**3**) was inactive against all cell lines, and the three trichoveroids (**III**), **2**, **9a**, and **9b**, were only active at the μM level. The remaining roridoids (**III**), **1a**, **1b**, **7a**, and **7b**, and the verrucaroid (**IV**), **6**, showed potent activity and cell selectivity. While each of these compounds exhibited slightly different activity patterns of Table 3 for CEM and the NCI leukemia cell against the different tumor types, in contrast to the pattern, in Table 3, the leukemia cell lines were less sensitive to these compounds. In comparing the results for the series **1a**, **1b**, **7a**, **7b** it would appear that the variations in the stereochemistry at C6′-C13′ are tolerated.

Conclusions

The sponge-derived strain of *Myrothecium verrucaria* examined here was rewarding to study as it elaborated a broad array of functionalized trichothecenes. Our strategy of saltwater culturing provided compounds in the trichoverroid (**II**), roridoid (**III**), and verrucaroid (**IV**) classes. By contrast, none of the previous studies, all involving culturing of *M. verucaria* in deionized water, has simultaneously provided compounds in each of these classes. An additional nuance on the chemical diversity of metabolites observed from our culture is that miophytocene C (**3**) was obtained, and it is distinctive in the absence of the C12−C13-epoxide normally present in a tricothecene. This observation mirrors a continuing theme observed in our laboratory wherein culturing known fungal strains in 100% seawater-based media can broaden the scope of the observed chemistry. However, it is now evident that some significant challenges need to be addressed in order to further develop this strategy as a useful means to expand marine natural products chemistry. Such efforts are ongoing in our laboratory and will be disclosed in the future.

The disk diffusion soft agar colony formation cytotoxicity data accumulated in this study may provide some additional insights on the potential of these structures for further therapeutic development. Consistent with previous trends, miophytocene C (**3**) is less potent because of the absence of the C12−C13 epoxide. Although anguidine (**17**) is intermediate in its relative activity, it is unselective. The best potency and, in some cases, the optimal murine leukemia tumor selectivity is associated with the presence of increased flexibility in the primed atoms (C1′ through C11′). For example, compounds possessing a 2′-OH in the macrocyclic ring of either a roridoid (**III**) or verrucaroid (**IV**) have increased relative activity, whereas the α,β unsaturated trichoveroids (**III**) (see **3** and **4**) are less active. Thus, the comparison of the relative activity levels of compounds **5** vs **6** and **8** vs **7a**/**7b** demonstrates that disruption of the conjugated chromophore at C1′-C3′ can be effective for increasing the potency. Severing of the macrocyclic ring (see **2**, **9a**, and **9b**) greatly reduces the relative activity. Turning to the issue of leukemia tumor selectivity, the best compounds in this regard are **7b**, **8**, and **9a**. However, the wide variations in their structures confound analysis of the requirements of their bioactivity. Finally, the therapeutic evaluation of selected active compounds is underway as **5**, **6**, **7a**, and **7b** are the subjects of pending in vivo studies and have also been selected for further investigation by the NCI Biological Evaluation Committee. We believe the results presented here along with the previous in vivo SAR patterns for anguidine (**17**) will assist in the further design of type **III** and **IV** class compounds for development as anticancer leads.

Experimental Section

General Experimental Procedures. UV/vis measurements were recorded on HP 8453 diode array spectrometer. Optical rotations were obtained on a JASCO DIP-370 digital polarimeter. The NMR spectra were recorded on a Varian

UNITY INOVA-500 spectrometer, operating at 500 and 125.7 MHz for ^1H and ^{13}C, respectively. High-resolution mass measurements were obtained on a benchtop Mariner ESI-TOF mass spectrometer. HPLC was performed with columns of 5 μm ODS.

Biological Materials. The fungus (strain no. 973023) was isolated following previously described techniques[40] from a *Spongia* sp.[41,42] (coll. no. 97103), identified by Dr. Cristina Diaz (UCSC, IMS), and collected using SCUBA off the coast of Maui in March 1997. The fungal culture was submitted for identification to Accugenix, a division of Acculabs, INS. The analysis, based on the alignment of the D2 region of the 25S ribosomal DNA compared against the MicroSeq database, identified the fungus as *Myrothecium verrucaria* with a genetic distance of 0.63%. A genetic distance of less than 1% is usually indicative of a species level match, however, data interpretation must be done on a case by case basis, taking into account the % GD (Genetic Distance) between known species closely related to other fungi. In addition, this fungus was identified as *Myrothecium verrucaria* from analysis of its fruiting body at the University of Texas Health Science Center at San Antonio. This fungus is maintained in a cryopreserved state at UCSC.

Culture Conditions. The fungal strain was grown in a liquid medium (12 L) containing 1.5% malt extract broth in filtered Monterey Bay seawater adjusted to pH 7.3 at 150 rpm for 21 days at room temperature (28 °C).

Disk Diffusion Soft Agar Colony Formation Assay. An in vitro cell-based assay was employed to identify solid tumor selectivity for original extracts, extract partition fractions, and pure compounds. The differential cytotoxicity[13b] is expressed by observing a zone differential between any solid tumor cell (Colon38, ColonH116, LungH125) and either leukemia cells (L1210 or CEM) or normal cells (CFU-GM). The sample is designated as "solid tumor selective" if (zone units of solid tumor−normal cell or leukemia cells) is greater than 250 units. The activity results appear in Tables 7, S2, and S3.

Extraction and Isolation. The culture was filtered under suction, and the broth was extracted with EtOAc thrice with equal volumes of EtOAc. The combined extract was evaporated to give a mixture of crude extract (E; 2.41 g). The organic extract was partitioned thrice between 10% aqueous MeOH and hexane. The aqueous MeOH soluble portion was further partitioned between 50% aqueous MeOH and CH_2Cl_2 thrice. The CH_2Cl_2 soluble extract (EFD; 1.64 g) was chromatographed on a silica gel column with CH_2Cl_2−MeOH as the eluent. The MeOH−CH_2Cl_2 (0:100), (1:99), (1:49), and (1:19) eluates were collected as two fractions [F1 (352.6 mg) and F2 (366.2 mg)], three fractions [F3 (146.9 mg), F4 (114.4 mg), and F5 (125.4 mg)], four fractions [F6 (123.9 mg), F7 (40.5 mg), F8 (169.7 mg), and F9 (142.6 mg)] and two fractions [F10 (76.2 mg) and F11 (16.2 mg)], respectively. F2 was purified by HPLC using MeOH−H_2O (1:1 up to 1:0) to give **6** (134.9 mg). F3 was purified by HPLC using MeOH−H_2O (7:3 up to 4:1) to yield **6** (15.1 mg) and **7a** (21.0 mg) and a fraction [F3H8 (21.0 mg)], respectively. F3H8 was purified by HPLC using MeCN−H_2O (1:1 up to 3:2) and gave **8** (3.7 mg) and **4** (7.6 mg), respectively. F4 was purified by HPLC using MeOH−H_2O (1:1 up to 1:0) and yielded **7a** (58.8 mg) and **5** (4.3 mg) and a fraction [F4H11 (4.2 mg)], respectively. F4H11 was purified by HPLC using MeCN−H_2O (4:1) to give **4** (1.0 mg). F5 was purified by HPLC using MeOH−H_2O (1:1 up to 1:0) to yield two fractions [F5H6 (21.0 mg) and F5H7 (22.4 mg)], respectively, and to give **1** (2.3 mg). F5H6 was purified by HPLC using MeCN−H_2O (2:3 up to 1:1) to give **1b** (13.5 mg) and **7b** (6.8 mg), respectively. F5H7 was purified by HPLC using MeOH−H_2O (3:2 up to 4:1) and gave **7a** (17.6 mg). F6 was purified by HPLC using MeOH−H_2O (13:7 up to 7:3) to yield a fraction [F6H9 (12.3 mg)]. F6H9 was purified by HPLC using MeCN−H_2O (9:11 up to 1:1) to give **2** (6.2 mg). F9 was purified by HPLC using MeOH−H_2O (3:2 up to 4:1) to yield two fractions [F9H7 (13.6 mg) and F9H8 (28.5 mg)], respectively. F9H7 was purified by HPLC using MeCN−H_2O (7:13 up to 9:11) to give **9b** (7.6 mg). F9H8 was purified by HPLC using MeCN−H_2O (7:13 up to 9:11) to give **9b** (4.1 mg) and **9a** (9.9 mg). F10 and F11 were combined and purified by HPLC using MeOH−H_2O (2:3 up to 4:1) to yield a fraction [F10, 11H17 (4.5 mg)]. F10, 11H17 was purified by HPLC using MeOH−H_2O (13:7 up to 3:1) to give **3** (2.8 mg). F10 and F11 were combined and purified by HPLC using MeOH−H_2O (3:2 up to 4:1) to yield a fraction [F10, 11H17 (4.5 mg)]. F10, 11H17 was purified by HPLC using MeOH−H_2O (13:7 up to 3:1) to give **3** (2.8 mg).

3-Hydroxyroridin E (1a): colorless powder. $[\alpha]^{27}_D$ −10.0° (*c*, 0.04, $CHCl_3$); UV (MeOH) λ_{max} (log ϵ) 262 nm (4.23); ^1H and ^{13}C NMR data see Table S5. HRESI-TOFMS: *m/z* 553.2420 $[M + Na]^+$ (calcd for $C_{29}H_{38}O_9Na$, 553.2408).

Roridin L (1b): colorless powder; $[\alpha]^{27}_D$ −28.6° (*c*, 0.14, $CHCl_3$); UV (MeOH) λ_{max} (log ϵ) 263 nm (4.53); ^1H and ^{13}C NMR data see Table S5. HRESI-TOFMS: *m/z* 553.2406 $[M + Na]^+$ (calcd for $C_{29}H_{38}O_9Na$, 553.2408).

13′-Acetyltrichoverrin B (2): colorless powder. $[\alpha]^{27}_D$ −45.5° (*c*, 0.13, $CHCl_3$); UV (MeOH) λ_{max} (log ϵ) 263 nm (4.80); ^1H and ^{13}C NMR data see Table S7. HRESI-TOFMS: *m/z* 597.2676 $[M + Na]^+$ (calcd for $C_{31}H_{42}O_{10}Na$, 597.2670).

Hydrolysis of 2. To a solution of 13′-acetyltrichoverrin B (**2**, 3.7 mg) in MeOH (2.0 mL) was added ammonium hydoxide (200 μL) at room temperature for 2 h with stirring. The reaction mixture was evaporated under reduced pressure to give a residue that was purified by a reversed-phase HPLC (60% up to 80% MeOH in H_2O, linear graient) to afford **9a** (2.9 mg). The ^1H and ^{13}C NMR spectra and the optical rotation ($[\alpha]^{27}_D$ −48.9°; *c*, 0.09, $CHCl_3$) of the reaction product were identical with **9a** isolated from the fungal extract. HRESI-TOFMS: *m/z* 555.2583 $[M + Na]^+$ (calcd for $C_{29}H_{40}O_9Na$, 555.2562).

Miophytocen C (3): colorless powder. $[\alpha]^{27}_D$ +8.8° (*c*, 0.25, $CHCl_3$); UV (MeOH) λ_{max} (log ϵ) 221 nm (4.22), 261 (4.06); ^1H and ^{13}C NMR data see Table S8. HRESI-TOFMS: *m/z* 569.2370 $[M + Na]^+$ (calcd for $C_{29}H_{38}O_{10}Na$, 569.2357).

Roridin M (4): colorless powder. $[\alpha]^{27}_D$ +42.1° (*c*, 0.19, MeOH); UV (MeOH) λ_{max} (log ϵ) 263 nm (4.96); ^1H and ^{13}C NMR data see Table S9. HRESI-TOFMS: *m/z* 551.2261 $[M + Na]^+$ (calcd for $C_{29}H_{36}O_9Na$, 551.2252).

Verrucarin M (5): colorless powder; $[\alpha]^{26}_D$ +32.1° (*c*, 0.06, $CHCl_3$); UV (MeOH) λ_{max} (log ϵ) 263 nm; ^1H and ^{13}C NMR data see Table S9; HRESI-TOFMS: *m/z* 501.2105 $[M + H]^+$ (calcd for $C_{27}H_{33}O_9$, 501.2119).

Verrucarin A (6): colorless powder. $[\alpha]^{27}_D$ +115.7° (*c*, 0.98, $CHCl_3$); HRESI-TOFMS: *m/z* 503.2280 $[M + H]^+$ (calcd for $C_{27}H_{35}O_9$, 503.2275). This compound was identified by comparison of spectral data with those of the literature values.[26]

Roridin A (7a): colorless powder. $[\alpha]^{27}_D$ +85.2° (*c*, 0.18, $CHCl_3$); HRESI-TOFMS: *m/z* 533.2760 $[M + H]^+$ (calcd for $C_{29}H_{41}O_9$, 533.2745). This compound was identified by comparison of spectral data with those of the literature values.[26]

Isororidin A (7b): colorless powder. $[\alpha]^{27}_D$ +68.3° (*c*, 0.08, $CHCl_3$); HRESI-TOFMS: *m/z* 555.2554 $[M + Na]^+$ (calcd for $C_{29}H_{40}O_9Na$, 555.2564). This compound was identified by comparison of spectral data with those of the literature values.[27]

Epiroridin E (8): colorless powder. $[\alpha]^{26}_D$ +15.2° (*c*, 0.07, $CHCl_3$); HRESI-TOFMS: *m/z* 515.2643 $[M + Na]^+$ (calcd for $C_{29}H_{39}O_8$, 515.2640). This compound was identified by comparison of spectral data with those of the literature values.[15a]

Trichoverrin A (9a): colorless powder. $[\alpha]^{26}_D$ −51.5° (*c*, 0.21, $CHCl_3$); HRESI-TOFMS: *m/z* 555.2560 $[M + Na]^+$ (calcd for $C_{29}H_{40}O_9Na$, 555.2565). This compound was identified by comparison of spectral data with those of the literature values.[28]

Trichoverrin B (9b): colorless powder. $[\alpha]^{27}_D$ −24.7° (*c*, 0.17, $CHCl_3$); HRESI-TOFMS: *m/z* 555.2551 $[M + Na]^+$ (calcd for $C_{29}H_{40}O_9Na$, 555.2565). This compound was identified by comparison of spectral data with those of the literature values.[28]

Acknowledgment. This work was supported by the National Institute of Health (RO1 CA 47135) Additional financial support at UCSC was provided by equipment grant from NSF BIR-94-19409 (NMR) and a supplement

to NIH CA 52955 for the purchase of the ESI-TOFMS. We thank Mr. Micheal Waddington, Accugenix, a division of Acculabs, INS, and Assistant Professor Deanna A. Sutton, Department of Pathology, University of Texas Health Science Center at San Antonio, for taxonomic identification for the fungus strain. We thank Dr. Cristina Diaz (UCSC, IMS) for the identification of the sponge taxonomy. We also thank Dr. David Newman (NCI) for providing anguidine.

Supporting Information Available: ^{1}H and ^{13}C NMR spectra and data of **1a**, **1b**, **2**, **3**, **4**, and **5**; bioassay results of extracts and fractions. This material is available free of charge via the Internet at http://pubs.acs.org.

References

(1) Kobayashi, M.; Uehara, H.; Matsunami, K.; Aoki, S.; Kitagawa, I. Trichoharzin, a New Polyketide Produced by the Imperfect Fungus *Trichoderma harzianum* Separated from the Marine Sponge *Micale cecilia*. *Tetrahedron Lett.* **1993**, *34*, 7925−7928.

(2) Cheng, X. C.; Varoglu, M.; Abrell, L. M.; Crews P.; Lobkovsky E.; Clardy J. Chloriolines A−C, Chlorinated Sesquiterpenes Produced by Fungal Cultures Separated from a *Jaspis* Marine Sponge. *J. Org. Chem.* **1994**, *59*, 6344−6348.

(3) Abrell, L. M.; Borgeson, B.; Crews, P. A New Polyketide, Secocurvularin, from the Salt Water Culture of a Sponge Derived Fungus. *Tetrahedron Lett.* **1996**, *37*, 8983−8984.

(4) Isolation: Varoglu, M.; Corbett, T. H.; Valariote, F. A.; Crews, P. Asperazine, a Selective Cytotoxic Alkaloid from a Sponge-Derived Culture of *Aspergillus niger*. *J. Org. Chem.* **1997**, 62, 7078−7079. (b) Synthesis: Govek, S. P.; Overman, L. E. Total Synthesis of Asperazine. *J. Am. Chem. Soc.* **2001**, *123*, 9468−9469.

(5) Isolation: Sperry, S.; Samuels, G. J.; Crews, P. Vertinoid Polyketides from the Saltwater Culture of the Fungus *Trichoderma longibrachiatum* Separated from a *Haliclona* Marine Sponge. *J. Org. Chem.* **1998**, 63, 10011−10014. (b) Synthesis: Wood, J. L.; Thompson, B. D.; Yusuff, N.; Pflum, D. A.; Matthäus, M. S. Total Synthesis of (±)-Epoxysorbicillinol. *J. Am. Chem. Soc.* **2001**, *123*, 2097−2098.

(6) Isolation: Amagata, T.; Doi, M.; Ohta, T.; Minoura, K.; Numata, A. Absolute Stereostructures of Novel Cytotoxic Metabolites, Gymnastatins A−E, from a *Gymnascella* Species Separated from a *Halichondria* Sponge. *J. Chem. Soc., Perkin Trans. 1* **1998**, *21*, 3585−3599. (b) Synthesis: Gurjar, M. K.; Bhaket, P. Total Synthesis of a Novel Metabolite Gymnastatin A. *Heterocycles* **2000**, *53*, 143−149.

(7) Lang, G.; Steffens, S.; Schaumann, K.; Bringmann, G. HPLC-UV, -MS, -NMR and -CD as Useful Tools in the Search for New Metabolites from Sponge Derived Fungi. *Scientific Programme, Book of Abstracts, List of Participants*; 3rd European Conference on Marine Natural Products, Elmau Castle, Bavaria, Sept 15−20, 2002; Munich, 2002, Abstract p 67.

(8) Ebel, R.; Lin, W. H.; Edrada, R. A.; Proksch, P. Biogenetically Diverse Secondary Metabolites from Sponge-Associated Fungi. *Scientific Programme, Book of Abstracts, List of Participants*; 3rd European Conference on Marine Natural Proudcts, Elmau Castle, Bavaria, September 15−20, 2002; Munich, 2002, Abstract, p 67.

(9) Smith, C. J.; Abbanat, D.; Bernan, V. S.; Maiese, W. M.; Greenstein, M.; Jompa, J.; Tahir, A.; Ireland, C. M. Novel Polyketide Metabolites from a Species of Marine Fungi. *J. Nat. Prod.* **2000**, *63*, 142−145.

(10) Höller, U.; Wright, A. D.; Matthée, G. F.; Konig, G. M.; Draeger, S.; Aust, H.-J.; Schulz, B. Fungi from Marine Sponges: Diversity, Biological Activity and Secondary Metabolites. *Mycol. Res.* **2000**, *104*, 1354−1365.

(11) Gautschi, J.; Valeriote, F. A.; Mooberry, S.; Crews, P. Looking Earlier and Deeper: Novel Metabolites from a Marine-Derived Fungus. *Program and Abstracts*; The 43rd Annual Meeting of the American Society of Pharmacognosy (ASP) and the 3rd Monroe Wall Symposium (MWS), New Brunswick, NJ, July 27−31, 2002; American Society of Pharmacognosy: New Brunswick, NJ, 2002; Abstract O-13, p 43.

(12) Ishibashi, M.; Iwasaki, T.; Imai, S.; Sakamoto, S.; Yamaguchi, K.; Ito, A. Laboratory Culture of the Myxomycetes: Formation of Fruiting Bodies of *Didymium bahiense* and Its Plasmodial Production of Makaluvamine A. *J. Nat. Prod.* **2001**, *64*, 108−110.

(13) Sperry, S.; Valeriote, F. A.; Corbett, T. H.; Crews, P. Isolation and Cytotoxic Evaluation of Marine Sponge-Derived Norterpene Peroxides. *J. Nat. Prod.* **1998**, *61*, 241−247. (b) Valeriote, F. A.; Grieshaber, C. K.; Media, J.; Pietraszkewicz, H.; Hoffman, J.; Pan, M.; McLaughlin, S. Discovery and Development of Anticancer Agents from Plants. *J. Exp. Ther. Oncol.* **2002**, *2*, 228−236.

(14) Jarvis, B. B. In *Mycotoxins and Phytoalexins in Human and Animal Health*; Sharma, R. P., Salunkhe, D. K., Eds.; CRC Press: Boca Raton, FL, 1991; pp 361−421. (b) Turner, W. B.; Aldridge, D. C. *Fungal Metabolites II*; Academic Press: New York, 1983; pp 228−238. (c) Cole, R. J.; Cox, R. H. *Handbook of Toxic Fungal Metabolites*; Academic Press: New York, 1981; pp 152−263.

(15) Jarvis, B. B.; Wang, S. Stereochemistry of the Roridins. Diasteromers of Roridin E. *J. Nat. Prod.* **1999**, *62*, 1284−1289. (b) Jarvis, B. B.; Wang, S.; Ammon, H. L. Trichoverroid Stereoisomers. *J. Nat. Prod.* **1996**, *59*, 254−261.

(16) Johannisson, A.; Björkhag, B.; Hansson, W.; Gadhasson, I.-L.; Thuvander, A. Effects of Four Trichothecen Mycotoxins on Activation Marker Expression and Cell Proliferation of Human Lymphocytes in Culture. *Cell Biol. Toxicol.* **1999**, *15*, 203−215.

(17) Zhou, H. R.; Harkema, J. R.; Hotchkiss, J. A.; Yan, D.; Roth, R. A.; Pestka, J. J. Lipopolysaccharide and the Trichothecene Vomitoxin (Deoxynivalenol) Synergistically Induce Apoptosis in Murine Lymphoid Organs. *Toxicol. Sci.* **2000**, *53*, 253−263.

(18) Isaka, M.; Punya, J.; Lertwerawat, Y.; Tanticharoen, M.; Thebtaranonth, Y. Antimalarial Activity of Macrocyclic Trichothecenes Isolated from the Fungus *Myrothecium verrucaria*. *J. Nat. Prod.* **1999**, *62*, 329−331.

(19) Garcia, C. C.; Rosso, M. L.; Bertoni, M. D.; Maier, M. S.; Damonte, E. B. Evaluation of the Antiviral Activity Against Junin Virus of Macrocyclic Trichothecenes Produced by the Hypocrealean Epibiont of *Baccharis cordifolia*. *Planta Med.* **2002**, *68*, 209−212.

(20) Breitenstein, W.; Tamm, C. Verrucarins Roridins. 34th Communication. Verrucarin K, the First Natural Trichothecene Derivative Lacking the 12, 13-Epoxy Group. *Helv. Chim. Acta* **1977**, *60*, 1522−1527. (b) Jarvis, B. B.; Vrudhula, V. M.; Midiwo, J. O.; Mazzola, E. P. New Trichoverroids from *Myrothecium verrucaria*: Verrol and 12,13-Deoxytrichodermadiene. *J. Org. Chem.* **1983**, *48*, 2576−2578. (c) Jarvis, B. B.; Midiwo, J. O.; Guo, M.-D. 12, 13-Deoxytrichoverrins from *Myrothecium verrucaria*. *J. Nat. Prod.* **1989**, *52*, 663−665. (d) Habermehl, G. G.; Busam, L.; Heydel, P.; Mebs, D.; Tokarnia, C. H.; Doebereiner, J.; Spraul, M. Macrocyclic Trichothecenes: Cause of Livestock Poisoning by the Brazilian Plant *Baccharis coridifolia*. *Toxicon* **1985**, *23*, 731−745. (e) Namikoshi, M.; Akano, K.; Meguro, S.; Kasuga, I.; Mine, Y.; Takahashi, T.; Kobayashi, H. A New Macrocytotoxic Trichothecene, 12, 13-Deoxyroridin E, Produced by the Marine-Derived Fungus *Myrothecium verrucaria*. *J. Nat. Prod.* **2001**, *64*, 396−398.

(21) Jarvis, B. B.; Midiwo, J. O.; Mazzola, E. P. Antileukemic Compounds Derived by Chemical Modification of Macrocyclic Trichothecenes. 2. Derivatives of Roridin A and H and Verrucarin A and J. *J. Med. Chem.* **1984**, *27*, 239−244.

(22) Fujimoto, Y.; Yokura, S.; Nakamura, T.; Morikawa, T.; Tatsuno, T. Total Synthesis of (±)-12, 13-Epoxytrichothec-9-ene. *Tetrahedron Lett.* **1974**, *29*, 2523−2526. (b) Brooks, D. W.; Grothaus, P. G.; Mazdiyasni, H. Total Synthesis of the Trichothecene Mycotoxin Anguidine. *J. Am. Chem. Soc.* **1983**, *105*, 4472−4473.

(23) Blackwell, B. A.; Miller, J. D.; Greenhalgh, R. ^{13}C NMR Study of Biosynthesis of Toxins by *Fusarium graminearum*. *J. Biol. Chem.* **1985**, *260*, 4243−4247.

(24) Trapp, S. C.; Hohn, T. M.; McCormic, S.; Jarvis, B. B. Characterization of the Gene Cluster for Biosynthesis of Macrocyclic Trichothecenes in *Myrothecium roridum*. *Mol. Gen. Genet.* **1998**, *257*, 421−432.

(25) Murakami, Y.; Okuda, T.; Shindo, K. Roridin L, M and Verrucarin M, New Macrocyclic Trichothecene Group Antitumor Antibiotics, from *Myrothecium verrucaria*. *J. Antibiot.* **2001**, *54*, 980−983.

(26) Breitenstein, W.; Tamm, C. ^{13}C NMR-Spectroscopy of the Trichothecane Derivatives Verrucarol, Verrucarins A and B and Roridins A, D and H. *Helv. Chim. Acta* **1975**, *58*, 1172−1180.

(27) Jarvis, B. B.; Midiwo, J. O. Stereochemistry of Roridins. *J. Nat. Prod.* **1982**, *45*, 440−448.

(28) Jarvis, B. B.; Stahly, G. P.; Pavanasasivam, G.; Midiwo, J. O.; Desilva, T.; Holmlund, C. E.; Mazzola, E. P.; Geoghegan, R. F. Isolation and Characterization of the Trichoverroids and New Roridins and Verrucarins. *J. Org. Chem.* **1982**, *47*, 1117−1124.

(29) Laurent, D.; Guella, G.; Roquebert, M.-F.; Farinole, F.; Mancini, I.; Pietra, F. Cytotoxins, Mycotoxins and Drugs from a New Deuteriomycete, *Acremonium neo-caledoniae*, from the Southwestern Lagoon of New Caledonia. *Planta Med.* **2000**, *66*, 63−66.

(30) Stessman, C. C.; Ebel, R.; Corvino, A. J.; Crews, P. Employing Dereplication and Gradient 1D NMR Methods to Rapidly Characterize Sponge-Derived Sesterterpenes. *J. Nat. Prod.* **2002**, *65*, 1183−1186.
(31) Iida, A.; Konishi, K.; Kubo, H.; Tomioka, K.; Tokuda, H.; Nishino, H. Trichothecinol A, B and C, Potent Anti-tumor Promoting Sesquiterpenoids from the Fungus *Trichothecium roseum*. *Tetrahedron Lett.* **1996**, *37*, 9219−9220.
(32) Wagenaar, M. M.; Clardy, J. Two New Roridins Isolated from *Myrothecium* sp. *J. Antibiot.* **2001**, *54*, 517−520.
(33) Kaneko, T.; Schmitz, H.; Essery, J. M.; Rose, W.; Howell, H. G.; O'Herron, F. A.; Nachfolger, S.; Huftalen, J.; Bradner, W. T.; Partyka, R. A.; Doyle, T. W.; Davies, J.; Cundliffe, E. Structual Modifications of Anguidin and Antitumor Activities of Its Analogues. *J. Med. Chem.* **1982**, *25*, 579−589.
(34) Corbett, T. H.; Griswold, D. P., Jr.; Roberts, B. J.; Peckham, J. C.; Schabel, F. M., Jr. Evaluation of single agents and combinations of chemotherapeutic agents in mouse colon carcinomas. *Cancer* **1977**, *40*, 2660−2680.
(35) Adler, S. S.; Lowenbraum, S.; Birch, B.; Jarrell, R.; Garrard J. Anguidine: A Broad Phase II Study of the Southeastern Cancer Study Group. *Cancer Treat. Rep.* **1984**, *68*, 423−425. (b) Goodwin, J. W.; Bottomley, R. H.; Vaughn, C. B.; Frank, J.; Pugh, R. H. Phase II Evaluation of Anguidine in Central Nervous System Tumors; A Southwest Oncology Group Study. *Cancer Treat. Rep.* **1983**, *67*, 285−286. (c) Bukowski, R.; Vaughn, C.; Bottomley, R.; Chen, T. Phase II Study of Anguidine in Gastrointestinal Malignancies: A Southwest Oncology Group Study. *Cancer Treat. Rep.* **1982**, *66*, 381−383. (d) Thigpen, J. T.; Vaughn, C.; Stuckey, W. J. Phase II Trial of Anguidine in Patients with Sarcomas Unresponsive to Prior Chemotherapy: A Southwest Oncology Group Study. *Cancer Treat. Rep.* **1981**, *65*, 881−882. (e) Yap, H.-Y.; Murphy, W. K.; DiStefano, A.; Blumenschein, G. R.; Bodey, G. P. *Cancer Treat. Rep.* **1979**, *63*, 789−791.
(36) Alvi, K. A.; Rabenstein, J.; Woodard, J.; Baker, D. D.; Bergthold, J. D.; Lynch, J.; Lieu, K. L.; Braude, I. A. 14′-Hydroxymytoxin B and 16-Hydroxyroridin E, Two New Cytotoxic Trichothecenes from *Myrothecium roridum*. *J. Nat. Prod.* **2002**, *65*, 742−744.
(37) Abbas, H. K.; Johnson, B. B.; Shier, W. T.; Tak, H.; Jarvis, B. B.; Boyette, C. D. Phytotoxicity and Mammalian Cytotoxicity of Macrocyclic Trichothecene Mycotoxins from *Myrothecium verrucaria*. *Phytochemistry* **2002**, *59*, 309−313.
(38) Sigg, H. P.; Mauli, R.; Flury, E.; Hauser, D. Structure of Diacetoxyscirpenol. *Helv. Chim. Acta* **1965**, *48*, 962−988.
(39) Boyd, M. R.; Pauli, K. D. Some Practical Considerations and Applications of the National-Cancer-Institute In-Vitro Anticancer Drug Discovery Screen. *Drug Dev. Res.* **1995**, *34*, 91−109.
(40) Varoglu, M.; Crews, P. Biosynthecally Diverse Compounds from a Saltwater Culture of Sponge-Derived *Aspergillus niger*. *J. Nat. Prod.* **2000**, *63*, 41−43.
(41) Bergquist, P. R. A Revision of the Supraspecific Classification of the Order Dictyoceratida, Dendroceratida, and Verongida (Class Demospongia). *New Zeal. J. Zool.* **1980**, *7*, 443−503.
(42) Bergquist, P. R. Dictyoceratida, Dendroceratida and Verongida from the New Caledonia Lagoon (Porifera: Demospongiae). *Mem. Queens. Mus.* **1995**, *38*, 1−51.

JM030090T